Metastable atomic configurations of Rh, Ir, and Pt on W(110)

J. Kolaczkiewicz
Institute of Experimental Physics, University of Wroclaw, Wroclaw PL 50-205, Poland

E. Bauer
Physikalisches Institut, Technische Universität Clausthal, D-3392 Clausthal-Zellerfeld, Federal Republic of Germany
(Received 19 February 1991)

The adsorption and structural rearrangement of Rh, Ir, and Pt on a macroscopic (110) single-crystal surface of W is studied as a function of coverage and temperature by low-energy electron-diffraction and work-function-change measurements. Long linear chains along the substrate ⟨111⟩ directions and tendency to order into a chain lattice are found. The linear structure is observed to be much more stable than on the small surfaces used in field-ion microscopy.

I. INTRODUCTION

The development of various forms of effective-potential calculations, for example, of the embedded-atom method[1,2] or the effective-medium theory[3] over the past seven years has made realistic simulations of atomic processes on surfaces possible and has stimulated renewed interest in the experimental study of this field. The theoretical models are most advanced for homonuclear systems which crystallize in the fcc structure and consequently recent experimental work has been directed mainly at such systems [Ir on Ir(100) (Refs. 4 and 5) and Ir(111) (Refs. 5 and 6)and Pt on Pt(100) (Ref. 7)]. The limitation to these high-melting point materials is mainly dictated by the experimental technique used, field-ion microscopy (FIM), which has been practically the sole source of information on atomic processes on well-defined metal surfaces up to now. This information has been restricted nearly exclusively to a few metals on W(110) and W(211) surfaces. (For reviews see Refs. 8–11.) One of the most surprising observations was that at low temperatures and small cluster size one-dimensional (1D) clusters, i.e., chains, were stable on the (110) surface instead of the expected two-dimensional (2D) configurations. The 1D clusters are always oriented along one of the ⟨111⟩ directions which is in accord with the strong anisotropy of the lateral interactions as derived from the pair distribution function.[12,13] Indirect electronic and elastic interactions have been invoked to explain this anisotropy but a full understanding is still lacking.

In order to achieve such an understanding the physical properties which determine chain formation must be understood better. These are electronic structure of adsorbate atoms and substrate, relative atomic radii r_A, r_S of adsorbate and substrate atoms, respectively (misfit), vibrational properties of adsorbate and substrate, and possibly others. Misfit does not seem to be a major parameter, at least as long as $r_A < r_S$, because chain formation is not only found for $r_A \approx r_S$, such as in Ir on Ir, Pt on Pt, or Pd on W and Mo but also when r_A is significantly smaller than r_S, for example, for Pd on Ta (Ref. 14) ($\Delta r/r_S = -3.9\%$) and for Ni on W (Ref. 15) ($\Delta r/r_S = -9.1\%$). For the case $r_A > r_S$ little information is available (Pt on W, $\Delta r/r_S = +1.2\%$) but it appears likely that the misfit is much less forgiving because of the anharmonicity of the adatom-adatom interaction potential.

The fact that clusters of a suitable size can be interconverted between 1D and 2D shapes merely by changing the annealing temperature suggests that vibrational properties should play a role but how is not clear at present. The most important factor, at least as judged on the basis of the available experimental data, appears to be the electronic structure of the adsorbate, while that of the substrate plays as little a role as the misfit does: Mo(110), W(110), and Ta(110), Ir(100) and Pt(100, and Ir(111) all are suitable substrates. The adsorbates Rh, Ir, Pd, and Pt show the strongest tendency to chain formation, much more so than Ni. Is this difference due to a difference in electronic structure or a consequence of the misfit difference? Is chain formation limited to the known cases or does it also occur in other adsorbates, such as Co or Au? What role does the *d*-level occupancy play?

Obviously these questions can be answered only by the study of other adsorbate-substrate systems, in particular, of other adsorbates. This requires additional techniques because of the main limitation of FIM: The high fields necessary for imaging exclude many substrates and adsorbates because of field desorption or field dissociation of the clusters. There are additional limitations which are connected with the small surface size which is needed in order to achieve quasiatomic resolution: (i) the number of adsorbate atoms is limited and as a consequence the number of possible configurations, (ii) the edge of the plane can act as a repulsive wall and influence the cluster configurations, or (iii) during the annealing steps used for equilibration atoms can be lost by diffusion off the edges.

Thus low- or zero-field methods which use large atomically flat surfaces are needed. Low-energy electron microscopy has shown that well-oriented macroscopic single-crystal surfaces have atomically flat areas with

linear extensions of 1 μm or more. (For a review see Ref. 16.) The distribution of adsorbate atoms on such a surface cannot only be imaged directly by a method with atomic resolution such as scanning tunneling microscopy but can also be obtained with laterally averaging methods: if there is some order, low-energy electron diffraction (LEED) is a powerful tool. If there is no order but a significant change in atomic distribution then work-function-change ($\Delta\phi$) measurements can be used as demonstrated for the *reversible* phase transition 2D condensate $\leftrightarrow$ 2D vapor[17,18].

In this paper, we use LEED and $\Delta\phi$ measurements in a study of the *irreversible* 1D$\rightarrow$2D cluster transition of Rh, Ir, and Pt on W(110). These three adsorbates were chosen because of their strong tendency to chain formation and their high 1D$\rightarrow$2D conversion temperature (350, 470, and 410 K, respectively[8,19]) which allows measurements at and above room temperature. The purpose of this paper is to demonstrate the feasibility and information content of the two methods for the present problem. Future work with improved experimental facilities such as specimen cooling and LEED spot profile analysis with a video LEED system will then address the questions asked earlier by studying other adsorbates on W(110) and on other surfaces not accessible to FIM. It is hoped that this study will stimulate theoretical work on the (110) surfaces of bcc metals for which realistic effective potentials are becoming available[2] so that the present limited understanding of atomic interactions on metal surfaces[7,11,18,20–22] will be broadened.

II. EXPERIMENT

The experiments were performed in a multimethod system equipped with LEED optics, an electron gun for $\Delta\phi$ measurements with the retarding field method, a cylindrical mirror analyzer for Auger electron spectroscopy (AES), a quadrupole mass spectrometer for thermal desorption spectroscopy (TDS), and several evaporators. The crystal was oriented by x-ray diffractometry to within 0.05° of the (110) orientation, was mechanically polished and cleaned *in situ* by extensive heating at 1400 K in 10^{-7} Torr oxygen, followed by flashing in ultrahigh vacuum to 2200 K to remove oxygen. After cleaning the ratio of the Auger electron signals of W:O and W:C were 1000:1 and 600:1, respectively. The base pressure was in the low 10^{-11} Torr range; during evaporation it rose into the high 10^{-11} Torr range and during the measurements it was about 4×10^{-11} Torr.

In the measurements reported here the crystal was heated indirectly from the backside by a bifilar Ta sheet heater up to a maximum temperature of 1200 K. For higher temperatures direct heating was used. The indirect heating was necessary in order to avoid magnetic-field disturbances in the $\Delta\phi$ measurement. The temperature was measured with a WRe thermocouple spotwelded to the crystal holder. The evaporators consisted of W wires onto which thin wires of Rh, Ir, and Pt were wrapped. Heating powers ranged from 15 W for Rh to 60 W for Ir. The radiation from the evaporators caused some heating of the W(110) crystal which limited the lowest accessible temperatures.

The dose sizes were calibrated in fractions of a monolayer (ML) which was determined by the breakpoint of the low-energy AES signals, the appearance of the TDS peak from the second ML, and the saturation of $\Delta\phi$ in high-temperature depositions or after annealing at high temperatures. $\Delta\phi$ was measured at about $\frac{1}{10}$ of the saturation current of the retarding field $I(V)$ curve of the clean surface. The TDS and AES results will be reported elsewhere[23] together with the LEED and $\Delta\phi$ data for higher coverages and temperatures. Here only the results of relevance for 1D clusters and the 1D$\rightarrow$2D cluster transition will be presented.

III. RESULTS

A. $\Delta\phi$ measurements

Figures 1–3 show the irreversible work-function changes observed during heating of layers with various

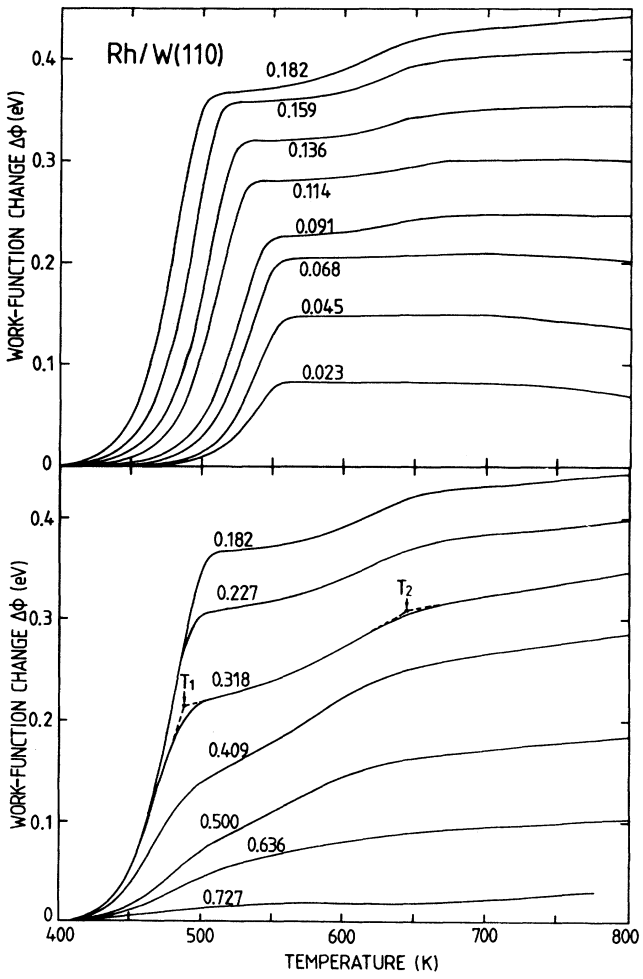

FIG. 1. Work-function change $\Delta\phi(T)$ during heating of a W(110) surface with various coverages (curve parameter) of Rh which was deposited at $T_0\approx350$ K. Heating rate 8 K s^{-1}. The definition of the temperatures T_1 and T_2 discussed in the text is shown for one curve.

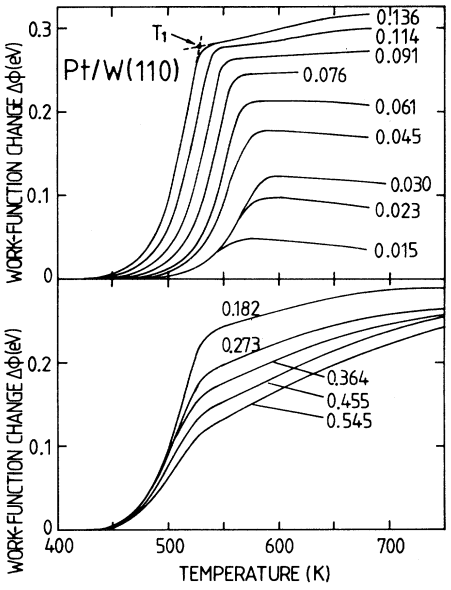

FIG. 2. Work-function change $\Delta\phi(T)$ during heating of a W(110) surface with various coverages of Pt which was deposited at $T_0 \approx 400$ K. Heating rate 4 K s^{-1}.

coverages at a constant heating rate of about 10 K s^{-1} which were deposited at temperatures T_0 of about 350 K (Rh) and 400 K (Pt, Ir). A strongly coverage-dependent rise of the work function to a first plateau-like level is found which is followed by a second, smaller rise which is best seen in Rh layers but also occurs for Pt and Ir, in the latter case at higher temperatures. Temperatures

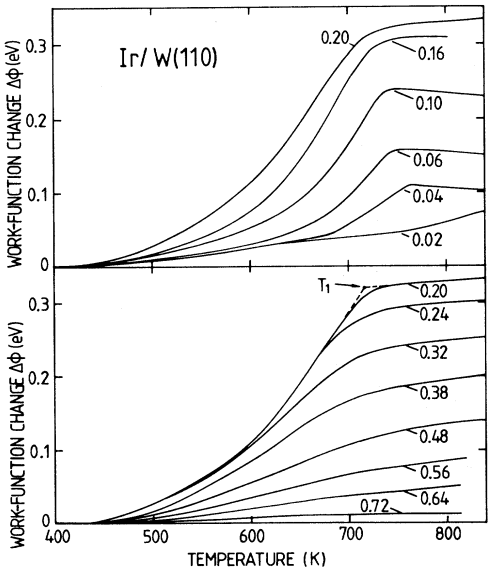

FIG. 3. Work-function change $\Delta\phi(T)$ during heating of a W(110) surface with various coverages of Ir which was deposited at $T_0 \approx 400$ K. Heating rate 7 K s^{-1}.

T_i $(i=1,2)$ can be defined (see Figs. 1–3) at which the structural changes causing the work-function changes are completed. The $\Delta\phi$ values $\Delta\phi_{T_i} - \Delta\phi_{T_0}$ are plotted in the lower parts of Figs. 4–6. Their upper part shows the work-function changes relative to the clean surface, in the case of Rh also the T_1 and T_2 values.

Although Rh, Ir, and Pt have larger electron affinities, electronegativities, and work functions than W, they cause a considerable decrease of the work function, a phenomenon well known from similar adsorbates (Pd, Au).[9] The differences $\Delta\phi_{T_1} - \Delta\phi_{T_0}$ are strongly coverage dependent and peak at $\Theta_M^{Rh} \approx 0.18$, $\Theta_M^{Ir} \approx 0.20$, and $\Theta_M^{Pt} \approx 0.11$ at 0.36, 0.30, and 0.28 eV, respectively. The data points for Ir show considerable scatter for two reasons: (i) specimen heating by radiation from the evaporator, (ii) incomplete desorption of Ir deposited in preceding experiments. Depending upon the size of a dose and the preceding dose — which were varied randomly in order to exclude systematic errors — the two effects were larger or smaller, causing the fluctuations seen within a sequence of depositions and between different depositions.

Several aspects of the results should be noted: (i) above T_1 the "plateau" is less and less pronounced with increasing coverage indicating a more or less continuous transition into the cluster configuration with higher work function. (ii) T_1 decreases with Θ up to Θ_M and then remains constant within the limits of error which is large at high

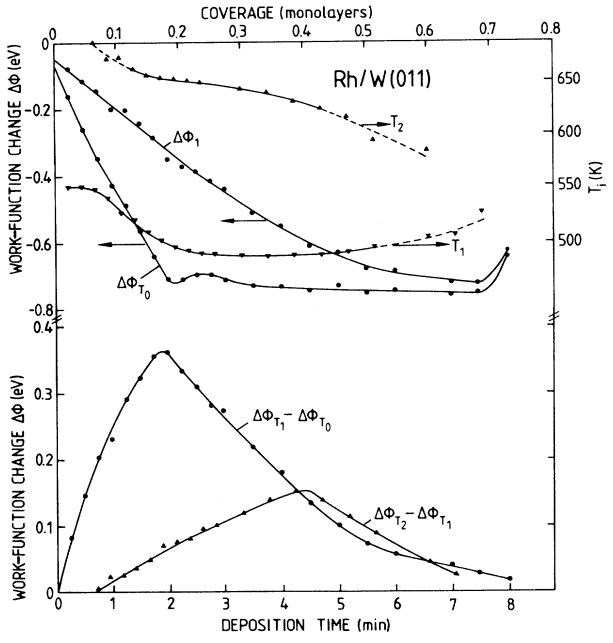

FIG. 4. Work-function change $\Delta\phi_{T_1}(\Theta) - \Delta\phi_{T_0}(\Theta)$ of a Rh-covered W(110) surface as a function of Rh coverage (bottom). The work function change $\Delta\phi_{T_0}(\Theta)$ upon deposition at T_0, the corresponding value $\Delta\phi_{T_1}(\Theta)$ at T_1 and the temperatures T_1 and T_2 are shown on top.

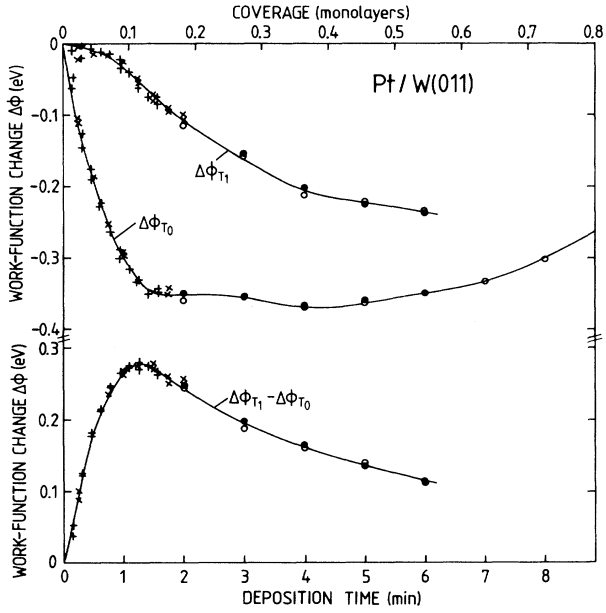

FIG. 5. Work-function changes $\Delta\phi_{T_0}(\Theta)$, $\Delta\phi_{T_1}(\Theta)$, and $\Delta\phi_{T_1}(\Theta)-\Delta\phi_{T_0}(\Theta)$ of a Pt-covered W(110) surface as a function of Pt coverage.

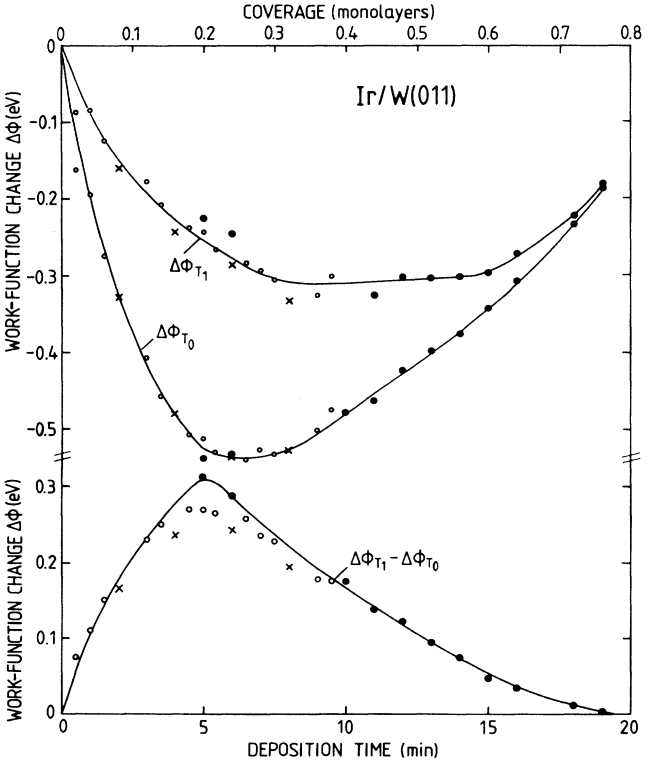

FIG. 6. Work-function changes $\Delta\phi_{T_0}(\Theta)$, $\Delta\phi_{T_1}(\Theta)$, and $\Delta\phi_{T_1}(\Theta)-\Delta\phi_{T_0}(\Theta)$ of a Ir-covered W(110) surface as a function of Ir coverage.

coverages (dashed lines). (iii) Below $\Theta\approx 0.02-0.04$ the work-function difference *per atom* between clusters at T_1 and clusters at T_0 is constant and then decreases. This suggests that below this coverage only one type of cluster exists and above it a mixture of T_1 and T_0 clusters, or that there is some depolarization in the T_0 clusters above this coverage.

B. LEED results

The LEED patterns of the three adsorbates show some similarities but also significant differences. At T_0 it consists of a (1×1) streak pattern [Fig. 7(a)] with a superimposed (3×1) spot pattern [Fig. 7(b)]. At $T\geq T_1$ the (3×1) spots have disappeared, the streaks have become much weaker or have contracted to the environment of the (1×1) spots [Fig. 7(c)]. Further heating makes the streaks disappear completely and satellite spots characteristic of the Kurdjumov-Sachs orientation appear which is expected for Rh, Ir, and Pt on W(110).[23] They are difficult to see at coverages $\Theta<0.2$ but definitely present at $\Theta\approx\frac{1}{4}$ and clearly visible at $\Theta\approx\frac{2}{3}$ after annealing at high temperatures [Fig. 7(d)]. The differences between the adsorbates are as follows: (i) The (1×1) streaks differ in sharpness, being sharpest for Pt and most diffuse for Ir. (ii) The relative intensity of the (3×1) spots to that of the (1×1) streaks is large for Rh and Ir but small for Pt. (iii) Certain (3×1) spots of Rh are systematically split; the (3×1) spots of Pt are too weak relative to the (1×1) streaks and those of Ir are too diffuse to allow such a statement. The poorer order of the Ir adsorbate very likely has to be attributed to the higher temperature during deposition which hindered the full development of the low-temperature cluster configuration. Therefore,

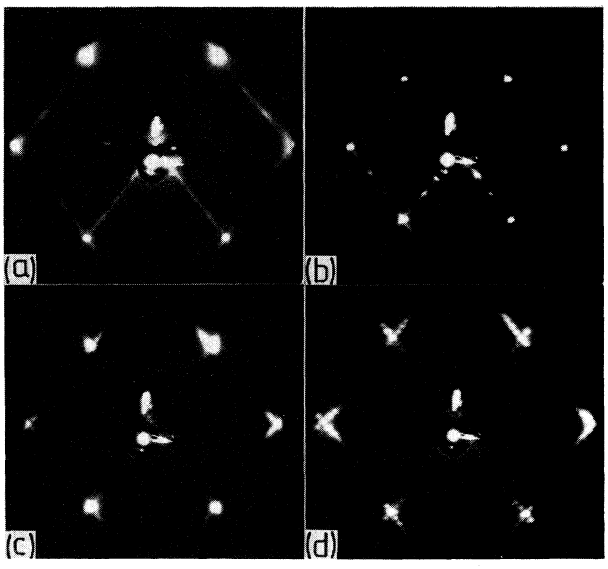

FIG. 7. LEED patterns of metal atom adsorbates on W(110). (a) Pt at $\Theta\approx\frac{1}{5}$ as deposited (45 eV), (b) Rh at $\Theta\approx\frac{1}{4}$ as deposited (73 eV), (c) Rh at $\Theta\approx\frac{1}{4}$ after annealing at $T<T_1$ (55 eV), (d) Rh at $\Theta\approx\frac{2}{3}$ after annealing at about 1200 K (48 eV).

only Rh and Pt will be examined more closely.

The (1×1) streaks are aligned along the $\langle 1\bar{1}2\rangle$ directions of the surface, that is, normal to the $\langle\bar{1}11\rangle$ directions. They are therefore attributed to one-dimensional diffraction of long adsorbate chains along the $\langle\bar{1}11\rangle$ directions. The half-width of the streaks is comparable to that of the substrate spots which is limited by the transfer width of the LEED system (≈ 100 Å). This implies chain lengths of about 40 atoms or more. The threefold periodicity along the streaks shows that there is a preferred threefold distance normal to the chains, that is, the $\langle\bar{1}11\rangle$ chains form a chain lattice, in particular in the case of Rh. Figure 7(b) shows that the (3×1) spots are split. The spots do not move with energy so that they cannot be attributed to faceting nor does the relative intensity of center and split spots oscillate with energy at a given coverage Θ and annealing temperature T_a. This means that the splitting is not caused by steps of islands of monoatomic height. The magnitude of the splitting and the intensity in the center do depend, however, somewhat on Θ and T_a.

All these observations can be explained by antiphase domain interference. Let $\mathbf{a}_1$ be the unit mesh vector in the chain direction ($\langle\bar{1}11\rangle$), $\mathbf{a}_2=\frac{1}{2}\langle 1\bar{1}1\rangle$ the other unit mesh vector and $\mathbf{b}_1$ and $\mathbf{b}_2$ the corresponding reciprocal unit mesh vectors. Consider two chain lattice islands with N_1 atoms per chain and N_2 chains and relative island displacement $\mathbf{d}=d_1\mathbf{a}_1+d_2\mathbf{a}_2$ within the coherence region of the instrument. Then the structure factor is

$$|F|^2=\frac{\sin^2(N_1\mathbf{K}\cdot\mathbf{a}_1/2)}{\sin^2(\mathbf{K}\cdot\mathbf{a}_1/2)}\frac{\sin^2(3N_2\mathbf{K}\cdot\mathbf{a}_2/2)}{\sin^2(3\mathbf{K}\cdot\mathbf{a}_2/2)}\cos^2(\mathbf{K}\cdot\mathbf{d}/2)\ . \tag{1}$$

Diffraction maxima [(3×1) spots] occur whenever $\mathbf{K}\cdot\mathbf{a}_1=2\pi h_1$ and $3\mathbf{K}\cdot\mathbf{a}_2=2\pi h_2$ or $\mathbf{K}_1/2\pi=h_1\mathbf{b}_1$ and $\mathbf{K}_2/2\pi=h_2\mathbf{b}_2/3$ (h_1,h_2 integers). For extinction of the center of the diffraction maximum by destructive interference between the two domains one must have $\mathbf{K}\cdot\mathbf{d}=(2n+1)\pi$ or

$$(h_1\mathbf{b}_1+h_2\mathbf{b}_2/3)\cdot(d_1\mathbf{a}_1+d_2\mathbf{a}_2)=h_1d_1+h_2d_2/3=(2n+1)/2\ .$$

For spots with even h_1+h_2 this implies $d_1=(2n+1)/4$, $d_2\approx 3(2n+1)/4$; for spots with odd h_1+h_2, $d_1=(2n+1)/2$, $d_2=3(2n+1)/2$. It is reasonable to assume that all atoms are adsorbed in equivalent high-symmetry sites (surface, lattice, bridge, on-top sites). The condition for odd h_1+h_2 cannot be fulfilled for any of these sites, the condition for even h_1+h_2 only for the surface sites (Fig. 8). The splitting of the spots with odd h_1+h_2 can be explained by double scattering between adsorbate and substrate which can be visualized by each diffracted beam from the substrate acting as incident beam on the layer. For example, the substrate (10) beam produces then the splitting of the $(0\ \frac{1}{3})$ spot (h_1+h_2 odd). The example shown in Fig. 8 ($n=0$) is unphysical because of the short distance between the sites. If $\mathbf{d}$ is restricted to within a (3×1) unit mesh then $n=1$ is the only possible choice. This case is illustrated in Fig. 9. It is interesting to note that only even n values give $\mathbf{d}$'s which interconnect the two types of surface sites. Thus the splitting of the $\frac{1}{3}$-order spots is an immediate consequence of the equivalence of the two surface sites indicated in Fig. 8 by dots. That the atoms of the chains are adsorbed in surface sites is not unexpected because isolated atoms have been found to be adsorbed usually in surface sites[8–13] although calculations for Cu, Ag, and Au place the site of strongest bonding closer to the lattice site.[24]

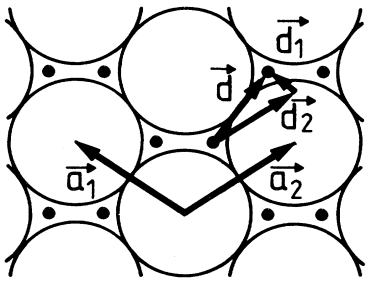

FIG. 8. Surface sites and (3×1) domain displacement vector $\mathbf{d}$ deduced from LEED spot splitting.

The 2D clusters obtained upon annealing are possibly pseudomorphic as long as they are small but a misfitting layer cannot be excluded without a detailed profile analysis of the (1×1) spots and their environment [Fig. 7(c)]. With increasing Θ and T_a, that is, increasing island size, these regions of the LEED pattern develop more

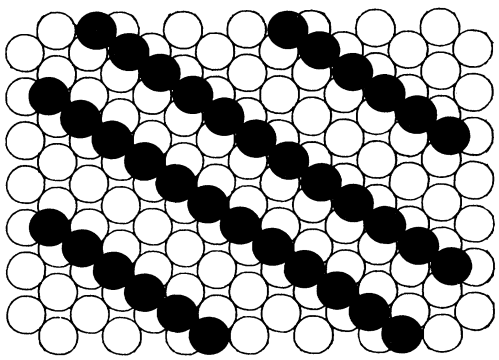

FIG. 9. (3×1) antiphase domain boundary for $n=1$. [$\mathbf{d}=3(\mathbf{a}_1+3\mathbf{a}_2)/4$.]

and more fine structure. For example, Fig. 7(d) shows satellites which indicate a hexagonal overlayer with an atomic spacing which is about 3% larger than in bulk Rh. The equilibrium structure of these layers will be discussed elsewhere[25] but the transition between the 1D and 2D structure requires still more detailed studies.

IV. DISCUSSION

The results reported in Sec. III demonstrate the usefulness of LEED and $\Delta\phi$ measurements for the study of metastable linear clusters and extend previous work done with FIM to larger surfaces and higher temperature. Larger surfaces are important because of the limitation of the possible cluster configurations by the small planes available in FIM and because of the temperature limitation due to diffusion of the adsorbate off the plane at temperatures above 350–400 K. Where the results overlap, good agreement is found with the FIM data. The tendency of Rh and Pt to form very long chains[8,19,26] in contrast to Ir which tends more to a mixture of 1D and 2D clusters[27] is confirmed here; likewise the transition from 1D to 2D clusters with increasing temperature. Also, the detailed analysis of the Θ and T_a dependence of $\Delta\phi$ gives quantitative data on activitation energies and prefactors of the processes involved in the 1D→2D cluster transition and other structural changes[25] although the nature of the processes cannot be identified in contrast to FIM. In addition, LEED shows that the chains can be much longer than the linear dimensions of the planes used in FIM and that the temperatures at which the 1D→2D transition is completed are much higher than deduced from FIM ($\approx$490, 530, and 700 K for Rh, Pt, and Ir, respectively). Of particular interest is the tendency of the chains to order in a chain lattice, increasing from Pt to Ir to Rh. This dependence upon the adsorbate suggests that the ordering is not so much a consequence of the instability of the substrate against periodic lattice distortions[28] but more likely caused by oscillating lateral interactions between the chains which favor a threefold periodicity. If the chain lattice could be grown in a single domain it would reach saturation coverage at $\Theta=\frac{1}{3}$. The observation that the maximum $\Delta\phi$ upon annealing is obtained at much lower coverage ($\Theta=0.11-0.20$) shows that 2D regions already form much earlier, presumably at the intersections of $\langle \bar{1}11 \rangle$ and $\langle 1\bar{1}1 \rangle$ chains as observed in FIM. In the case of Rh the (3×1) structure can be seen already at very small coverages ($\Theta\approx0.05$). This suggests island formation which requires a surprisingly strong attractive interaction at three atomic distances, a challenge to theory. Long narrow islands in only one of two equivalent orientations have been observed on a much larger scale in 2D islands of Au on W(110) by low-energy electron microscopy (see, e.g., Fig. 12.11a in Ref. 16). It would be interesting to examine if large chain lattice regions in only one orientation can also be grown in order to understand this unusual long-range order of atomically flat terraces.

V. SUMMARY

We have shown that two simple and well-established experimental methods, LEED and $\Delta\phi$ measurements, can be used to obtain detailed information on 1D clusters and on the transition to 2D clusters with increasing coverage and temperature. This opens up the possibility of studying a much wider variety of adsorbates and substrates than those accessible to FIM. It is hoped that such studies will lead to a better understanding of this one-dimensional order which is possible only due to the ordering field of the substrate.

ACKNOWLEDGMENT

This work was supported by the Deutsche Forschungsgemeinschaft.

[1]M. S. Daw and M. I. Baskes, Phys. Rev. B **29**, 6443 (1984).
[2]J. B. Adams and S. M. Foiles, Phys. Rev. B **41**, 3316 (1990), and references cited therein.
[3]K. W. Jacobsen, J. K. Nørskov, and M. J. Puska, Phys. Rev. B **35**, 7423 (1987).
[4]P. R. Schwoebel and G. L. Kellogg, Phys. Rev. Lett. **61**, 578 (1988).
[5]C. Chen and T. T. Tsong, J. Phys. (Paris) Colloq. **50**, C8-273 (1989); Phys. Rev. B **41**, 12 403 (1990).
[6]S. C. Wang and G. Ehrlich, Surf. Sci. **217**, L397 (1989).
[7]P. R. Schwoebel, S. M. Foiles, C. L. Bisson, and G. L. Kellogg, Phys. Rev. B **40**, 10 639 (1989).
[8]D. W. Bassett, in *Surface Mobilities on Solid Materials,* edited by V. T. Vinh (Plenum, New York, 1983), pp. 63 and 83.
[9]E. Bauer, in *The Chemical Physics of Solid Surfaces and Heterogeneous Catalysis,* edited by D. A. King and D. P. Woodruff (Elsevier, New York, 1984), Vol. 3, p. 1.
[10]G. Ehrlich, in *Chemistry and Physics of Solid Surfaces,* edited by R. Vanselow and R. Howe (Springer, Berlin, 1984), Vol. 5, p. 283.
[11]T. T. Tsong, Rep. Prog. Phys. **51**, 759 (1988); Surf. Sci. Rep. **8**, 127 (1988).
[12]H. -J. Krause, M. S. thesis, Technische Universität Clausthal, 1981.
[13]F. Watanabe and G. Ehrlich, Phys. Rev. Lett. **10**, 1146 (1989).
[14]P. R. Schwoebel and G. L. Kellogg, Phys. Rev. B **38**, 5326 (1988).
[15]G. L. Kellogg, Surf. Sci. **187**, 153 (1987), and references cited therein.
[16]E. Bauer, in *Chemistry and Physics of Solid Surfaces,* edited by R. Vanselow and R. Howe (Springer, Berlin, 1990), Vol. 8, p. 267 and references cited therein.
[17]J. Kolaczkiewicz and E. Bauer, Phys. Rev. Lett. **53**, 485 (1984); Surf. Sci. **151**, 333 (1985).
[18]E. Bauer, Appl. Phys. A **51**, 71 (1990).
[19]V. R. Dhanak and D. W. Bassett, Surf. Sci. **238**, 289 (1990).
[20]P. R. Schwoebel and P. J. Ferbelman, Surf. Sci. **216**, 263 (1989).
[21]A. F. Wright, M. S. Daw, and C. Y. Fong, Phys. Rev. B. **42**, 9409 (1990).
[22]G. W. Jones, J. M. Marcano, J. N. Nørskov, and J. A. Venables, Phys. Rev. Lett. **65**, 3317 (1990).

[23]E. Bauer and J. H. van der Merwe, Phys. Rev. B **33**, 3657 (1986), and references cited therein.
[24]H. Gollisch, Surf. Sci. **175**, 249 (1986).
[25]J. Kolaczkiewicz and E. Bauer (unpublished).
[26]G. L. Kellogg and P. R. Schwoebel, Surf. Sci. **224**, 489 (1989).
[27]D. W. Bassett and D. R. Tice, Thin Solid Films **20**, S37 (1974).
[28]R. H. Gaylord, K. H. Jeong, and S. D. Kevan, Phys. Rev. Lett. **62**, 2036 (1989).

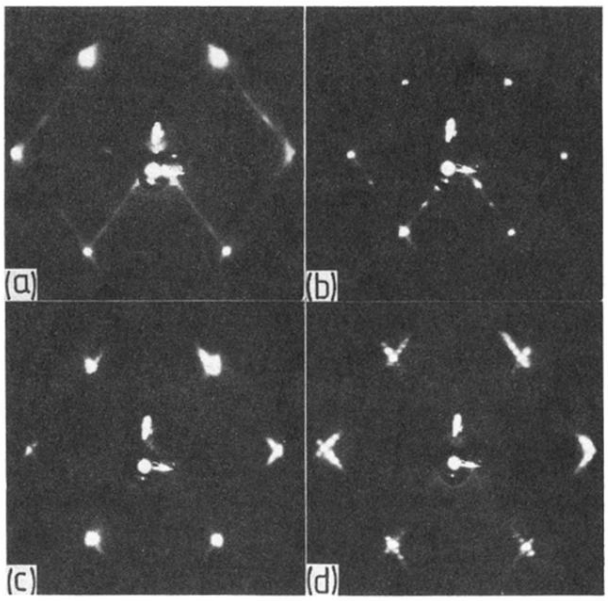

FIG. 7. LEED patterns of metal atom adsorbates on W(110). (a) Pt at $\Theta \approx \frac{1}{5}$ as deposited (45 eV), (b) Rh at $\Theta \approx \frac{1}{4}$ as deposited (73 eV), (c) Rh at $\Theta \approx \frac{1}{4}$ after annealing at $T < T_1$ (55 eV), (d) Rh at $\Theta \approx \frac{2}{3}$ after annealing at about 1200 K (48 eV).